Mathematics and Statistics 10(5): 925-935, 2022 http://www.hrpub.org
DOI: 10.13189/ms.2022.100504

Stochastic-Fractal Analysis Modeling of Salts Precipitation from Aqueous Solution

Isela J. Reyna-Rosas[1], Josué F. Pérez-Sánchez[2], Edgardo Suárez-Domínguez[2,*], Alejandra Hernández-Alvarado[1], Susana Gonzalez-Santana[3], F. Izquierdo-Kulich[3]

[1]Facultad de Arquitectura, Diseño y Urbanismo, Universidad autónoma de Tamaulipas, Circuito Interior S/N, Tampico, Tamaulipas, CP 89000, Mexico
[2]FADU Research Centre, Centro Universitario Sur, UAT. Circuito Interior S/N. Tampico, Tamaulipas, CP 89506, Mexico
[3]Universidad de la Habana, Calle Zapata s/n, entre G y Carlitos Aguirre, Vedado, CP 10400, Cuba

Received May 17, 2022; Revised August 8, 2022; Accepted August 30, 2022

Cite This Paper in the Following Citation Styles

(a): *[1] Isela J. Reyna-Rosas, Josué F. Pérez-Sánchez, Edgardo Suárez-Domínguez, Alejandra Hernández-Alvarado, Susana Gonzalez-Santana, F. Izquierdo-Kulich , "Stochastic-Fractal Analysis Modeling of Salts Precipitation from Aqueous Solution," Mathematics and Statistics, Vol. 10, No. 5, pp. 925 - 935, 2022. DOI: 10.13189/ms.2022.100504.*

(b): *Isela J. Reyna-Rosas, Josué F. Pérez-Sánchez, Edgardo Suárez-Domínguez, Alejandra Hernández-Alvarado, Susana Gonzalez-Santana, F. Izquierdo-Kulich (2022). Stochastic-Fractal Analysis Modeling of Salts Precipitation from Aqueous Solution. Mathematics and Statistics, 10(5), 925 - 935. DOI: 10.13189/ms.2022.100504.*

Abstract Electrolytes are of interest because thin plate coatings are normally obtained from aqueous solutions. The properties of the surface are important because various properties such as resistance or durability depend on it. To understand the phenomenological processes, it is better to analyze simpler processes such as sodium chloride. In this paper, a model is proposed to predict the temporal behavior of the fractal dimension of the patterns formed in salts precipitation by solvent evaporation in a scattering surface; for fractal-box counting, ImageJ software was used. The model was obtained by applying stochastic methods and fractal geometry, describing the internal fluctuations caused by precipitation and dissolution on the mesoscopic scale of solid crystalline particles. From adjusting the proposed model to the experimental data, it is possible to estimate the velocity constants related to the microscopic precipitation processes of the particles that form the pattern. The model was validated and used to study the precipitation of carbonate salts and sodium chloride, respectively, obtaining predictions corresponding to the physicochemical properties of these salts. From the adjustment of the proposed models to the observed experimental data, the value of the velocity constants of the precipitation and dissolution processes was also estimated.

Keywords Ionic Interactions Model, Fractal Dimension Application, Stochastic Precipitation-Diffusion Processes

1. Introduction

Electrolytes are cells that dissociate into ions in the presence of a solvent. The degree of dissociation, representing the fraction of molecules that dissociate, depends on the solvent and the electrolyte [1]. When the degree of dissociation is near to one, these substances are classified as strong electrolytes, while significantly lower ones correspond to weak electrolytes [2].

The presence of ions in a solution affects the solvent-solvent stability, as the electric charge attracts solute molecules through ion-dipole interactions, causing the solvation of the ions (Figure 1). This process is known as the hydration of ions for aqueous electrolyte solutions [3]. Ionic hydration increases the effective size of the ions, with the consequent decrease in their mobility and the speed of the processes associated with their migration and diffusion [3,4]. As the concentration of the ions increases, the oppositely charged ions are more likely to bind, causing the electrolyte to precipitate. As ionic hydration turns higher, the precipitation of hydrates also occurs [5].

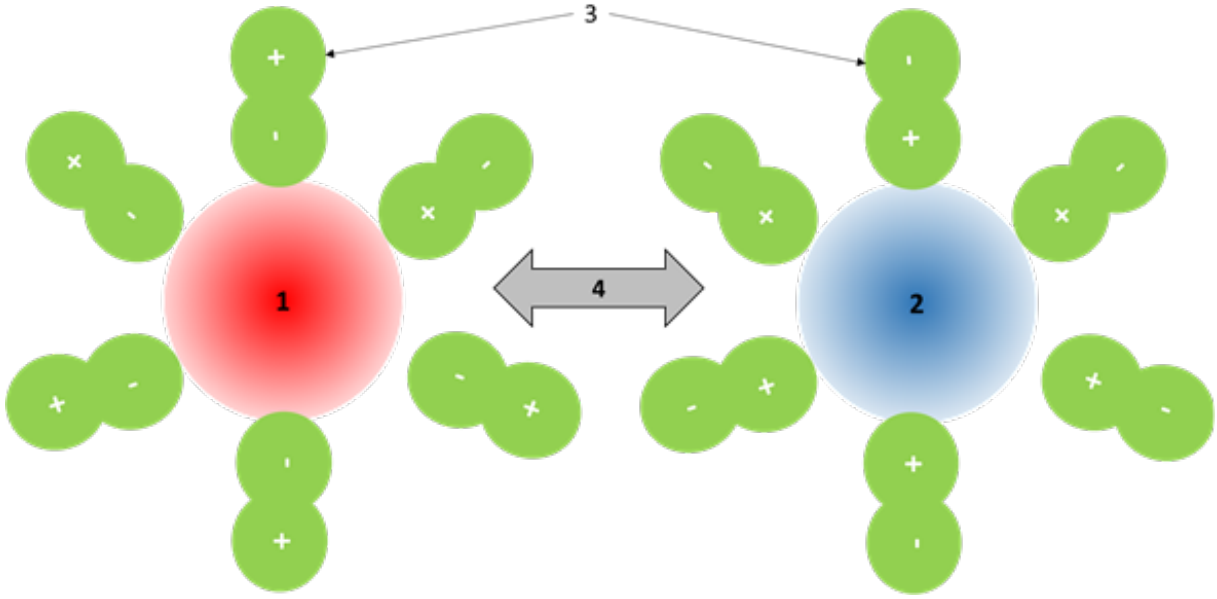

Figure 1. Solvation of ions: 1: positive ion A+; 2: negative ion B- ; 3: solvent molecules; 4: electrostatic interaction forces that are established between ions of opposite charge

When the aqueous solution of salt AB is spreading on a surface, water evaporates through time, which leads to the increase of the ionic concentration with the consequent precipitation of the salt. This phenomenon involves the occurrence of transport processes associated with the diffusion and migration of ions, as well as chemical processes related to the formation and precipitation of salt, where the stoichiometry of precipitate formation is represented as [6]:

$$A^{+}_{(aq)} + B^{-}_{(aq)} \rightarrow AB_{(s)}$$

The precipitated particles have different sizes and shapes and are distributed on the surface forming a complex pattern that depends on the chemical and transport processes that take place, respectively, as well as the conditions of the system [7].

The arrangement of ions can be reproduced by stochastic analysis [8] while the shapes of solid crystals are best explained by fractal geometry [9].

Such behaviors are relevant for areas like engineering, architecture, and construction [10] since it has been proven that crystallization processes are responsible for the cracking of soils [11] and concrete [12] in addition to damaging some structures based on earth-based construction technologies that have a greater potential for housing development [13].

The aspects presented in this research are related to the theoretical and experimental study of the pattern's morphogenesis. The objectives consisted of 1) obtaining a mesoscopic model to describe the precipitation process; 2) obtaining a theoretical expression to characterize the temporal evolution of crystallization patterns through the fractal dimension, and 3) comparing the theoretical results obtained with the experimental results observed to validate the proposed mathematical model.

2. Methods

2.1. Obtaining the Mesoscopic Model and Estimating the Fractal Dimension

From the microscopic point of view, the processes associated with the binding of ions and the formation and dissolution of solid particles occur with a certain probability associated with thermal fluctuations and the diffusion processes of the different chemical species [8]. As a result, solid particles precipitated during the evaporation of water have a diversity of sizes and shapes, and are randomly distributed on the surface, forming a spatial pattern that cannot be described by Euclidean geometry, being more appropriate the use of fractal geometry.

For describing the morphogenesis process, a mesoscopic model describes the temporal behavior of the observed surface area covered by the solid particles and of the variance associated with the internal fluctuations of the particles' precipitation random processes. For this purpose, the following considerations were established:

(i). The observed system is the surface area A on which the precipitation of salts occurs.

(ii). The microscopic variable that describes the system is the number of precipitated solid particles n, which size is characterized by the average area α that an individual particle projects onto the observed surface. In this case, it is assumed that all the particles have the same size and are equal to the average, which is a

necessary approximation to simplify the mathematical treatment related to obtaining the model.

(iii). The macroscopic variable considered is the fraction ϕ of the area occupied by the particles so that the relationship between the microscopic and macroscopic variables is given by:

$$\phi = \frac{n\alpha}{A} \tag{1}$$

(iv). The microscopic processes assumed are a) the increment *n+1* due to the union of ions and precipitation of a particle, whose probability of transition per unit of time W_1 is considered proportional to the number of *particles m* that are dissolved and is considered *a priori*:

$$W_1 = km \tag{2}$$

And b) the decrease *n-1* due to the dissolution of the solid particle in water, whose transition probability per unit of time W_2 is:

$$W_2 = gn \tag{3}$$

For equations (2) and (3), k and g represent the velocity constants associated with the precipitation and dissolution processes. The values of these parameters depend on the nature of the electrolyte and the electrostatic interaction forces experienced by the ions, as well as the molecular interactions of these with the solvent molecules, among other factors, such as the conditions of the system (temperature and pressure) and the speed of diffusion of the chemical species that are present. The theoretical estimation of these parameters turns out to be complex, therefore, their determination must be made experimentally. There are other ways to solve the equations, as mentioned in [14]. In this case we use some derived from stochastic equations like what is explained below.

From the microscopic processes considered, the master equation [15] is obtained, which describes the behavior of the probability $P(n,t)$ of n particles precipitated at time t:

$$\begin{aligned} &\frac{\partial P(n;t)}{\partial t} = \left(\mathbf{E}^{-1} - 1\right)kmP(n;t) + \left(\mathbf{E}^{+1} - 1\right)gnP(n;t) \\ &P(n_0;0) = 1 \end{aligned} \tag{4}$$

where **E** is the ascent-descent operator acting on the functions of discrete variables. In this equation, the left term represents the non-stationary behavior considering the macroscopic time scale, while on the right side the probabilities of transition per unit of time implicitly involve time on the microscopic scale.

From the master equation (4) and the relationship between the microscopic and macroscopic variables, the equivalent Fokker - Planck equation expressed as a function of the observed macroscopic variable is obtained:

$$\begin{aligned} &\frac{\partial P(\phi;t)}{\partial t} = -\frac{\partial}{\partial \phi}kM_0P(\phi;t) + \frac{1}{2\Omega}\frac{\partial^2}{\partial \phi^2}(kM_0 + g\phi)P(\phi;t) \\ &P(\phi_0;0) = 1 \end{aligned} \tag{5}$$

where:

$$\Omega = \frac{\alpha}{A} \tag{6}$$

is the scaling factor relating the size of the particles and the size of the observed system. Eq. (5) and (6) define the magnitude of the internal fluctuations (the fluctuations in a particle will be greater as the size of the observed system decreases), whereas

$$M_0 = \frac{m\alpha}{A} = \frac{C_0V}{\rho\upsilon}\frac{\alpha}{A} \tag{7}$$

represents the area fraction that would be occupied by the dissolved particles if they precipitate, being C_0 (kg/m^3) the initial concentration of the electrolyte, V (m^3) the initial volume of the electrolytic solution, ρ (kg/m^3) the density of the solid particles and υ (m^3) the volume of an individual solid particle.

Equation (5) is a linear equation so that its solution is a normal distribution function [16]:

$$P(\phi;t) = \frac{1}{\sqrt[2]{2\pi\sigma(t)}}\exp\left(-\frac{(\phi - \Phi(t))^2}{2\sigma(t)}\right) \tag{8}$$

where the expected value Φ of ϕ and the variance σ of the internal fluctuations that occur around this value due to the stochastic nature of the processes, evolve and are described through the system of differential equations:

$$\frac{d\Phi}{dt} = kM_0 - g\Phi \tag{9}$$

$$\frac{d\sigma}{dt} = -2g\sigma + \frac{1}{\Omega}(kM_0 + g\Phi) \tag{10}$$

subject to boundary conditions:

$$\begin{aligned} \Phi(0) &= \Phi_0 \\ \sigma(0) &= 0 \end{aligned} \tag{11}$$

and whose exact analytical solution is given by:

$$\Phi = \frac{kM_0}{g} + \left(\Phi_0 - \frac{kM_0}{g}\right)\exp(-gt) \tag{12}$$

$$\sigma(t) = \frac{1}{\Omega}\left(\left(\Phi_0 - \frac{kM_0}{g}\right)\exp(-gt) - \Phi_0\exp(-2gt) + \frac{k}{g}M_0\right) \tag{13}$$

Equations (12) and (13) represent the temporal behavior of the observed variables and fully describe the behavior of the system because the probability function is normal or Gaussian [17].

2.2. Estimation of the Fractal Dimension

It is considered that the internal fluctuations that are present in the system are responsible for the random and irregular spatial pattern shown by the precipitated particles, so to obtain an expression that estimates the value of their fractal dimension, the mesoscopic model is applied. This approach has successfully described patterns associated with different physical, chemical, and biological phenomena. The probability is considered from the bulk scale, and the relationship between matter and the fractal dimension [18].

For the characterization of the formed pattern, the system is "frozen" in time. It is assumed that changes in the expected value during the observation time can be considered negligible. The system is supposed to be in a "quasi-stationary state". In this way, making equal to zero the time derivative involved in equations (8) and (9) it is obtained:

$$\Phi = \frac{kM_0}{g} \tag{14}$$

$$\sigma = \frac{1}{2\Omega}\left(\Phi + \frac{kM_0}{g}\right) \tag{15}$$

Suppose the probability P (() is visualized from the point of view of the bulk scale [17]. The density of substance ψ present in the system can be estimated from the expected value of the probability:

$$\psi = \int P(\Phi)P(\Phi)d\Phi = C\frac{1}{\sqrt[2]{\sigma}} = C\frac{1}{\sqrt[2]{\frac{1}{2\Omega}\left(\Phi + \frac{kM_0}{g}\right)}} \tag{16}$$

On the other hand, according to the definition of fractal dimension, the amount of substance contained in a two-dimensional system is defined by Ψ [19]:

$$\Psi = Cl^{f} = \int\int \psi dldl \tag{17}$$

where l is the Euclidean distance between two spatial points so that this distance is proportional to the size of the observed system. For fractal dimension, the fraction of area is represented as:

$$\Phi = l^2 \tag{18}$$

and equation (16) is expressed as a potential function of l, where the value of the power u is [18]:

$$u = \lim_{l\to 1}\left(\frac{d\ln C\frac{1}{\sqrt[2]{\frac{1}{2\Omega}\left(l^2+\frac{kM_0}{g}\right)}}}{dl}\left(\frac{d\ln l}{dl}\right)^{-1}\right) \tag{19}$$

$$u = -\frac{g}{g + kM_0}$$

in such a way that

$$\psi = Cl^{u} \tag{20}$$

and

$$\Psi = Cl^{f} = \int\int Cl^{u} dldl = Cl^{u+2} \tag{21}$$

In equations (16), (17), (20), and (21), the parameter C represents the integration constant. Comparing equations (17) and (21) it is obtained:

$$f = 2 - \frac{g}{g+kM_0} = \frac{1+2\frac{kM_0}{g}}{1+\frac{kM_0}{g}} \tag{22}$$

Substituting equation (14) in equation (22) results in the relationship between the fractal dimension and the area fraction covered by the particles:

$$f = \frac{1+2\Phi}{1+\Phi} \tag{23}$$

If it is considered that $\Phi << 1$, then a linear relationship is obtained between the fractal dimension and a fraction of the covered area:

$$f = 1 + 2\Phi \tag{24}$$

Equation (24) is a theoretical relationship that allows estimating the value of the fractal dimension as a function of the fraction of area obtained when an observation of the system is made. In this sense, it must be considered that the value of the fractal dimension determined experimentally, as well as the fraction of area covered, requires converting a 2D image of the system under study into a binary image that reflects the spatial pattern formed. There are different ways to visualize this pattern depending on its complexity and image noise level. For this reason, it is more realistic to define a linear relationship:

$$f = \beta_0 + \beta_1\Phi \tag{25}$$

where the values of β_0 and β_1 are determined from the statistical adjustment of the experimental results obtained.

The area fraction covered by the precipitated particles evolves in time according to equation (12), then substituting (12) in (24), and an equation is obtained that allows estimating the temporal behavior of the fractal dimension:

$$f = \phi_0 + \phi_1\, exp(-gt) \tag{26}$$

where parameters φ_0, φ_1, and g are statistically adjusted to the observed experimental values. These parameters are related to the parameters involved in the proposed theoretical model, from the relationships:

$$\phi_0 = \beta_0 + \frac{kM_0}{g}\beta_1 \tag{27}$$

$$\phi_1 = \left(\Phi_0 - \frac{kM_0}{g}\right)\beta_1 \tag{28}$$

3. Materials and Methods

Two salt precipitation experiments were conducted to obtain the experimental results from aqueous solutions of

sodium chloride (NaCl) and calcium carbonate ($CaCO_3$). The concentration used in each experiment and the solubility of each salt are shown in Table 1.

Table 1. Salt concentration and solubility of this used to carry out the experiments

Experiment	Salt	Concentration (g/l)	Solubility (g/l)
1	NaCl	360	350
2	$CaCO_3$	0.0031	0.013

A drop of each solution was spread over a glass slide, and pictures of the pattern formed by the precipitated salts for different time values were obtained using a CELESTRON digital microscope (x1000). Each image was transformed to a binary image. The pattern formed by the precipitation corresponds to the interface between the particle and the solvent, shown in Figure 2. The area fraction covered for each binary image and the fractal dimension was determined using the box-counting method. The particles size distribution was measured considering the perimeter (pixels) and the average area of each particle (pixels^2), in such a way that the average specific surface area (pixels) / (pixels^2), can be estimated as equivalent to the quotient between the average and the area. All image processing was done using the ImageJ software.

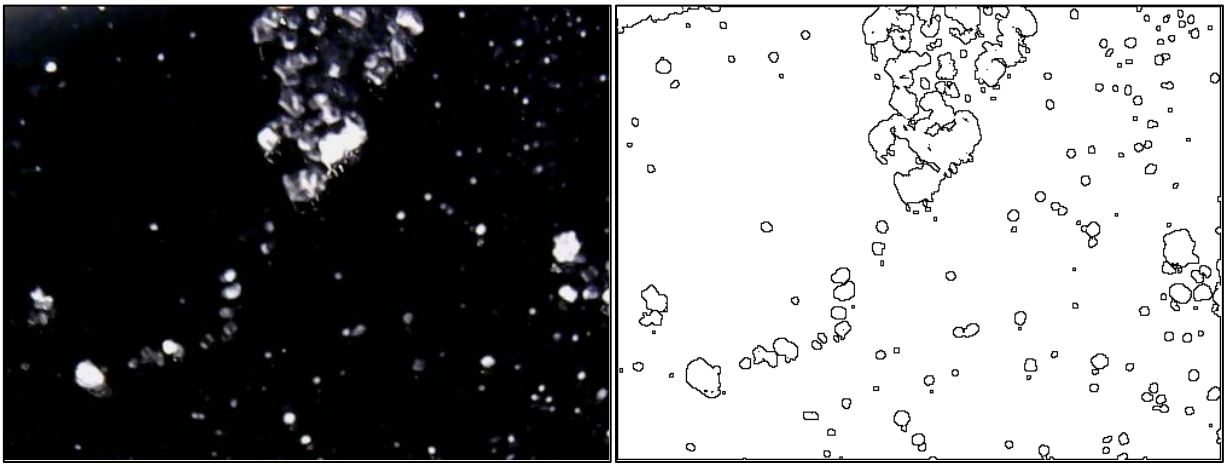

a)

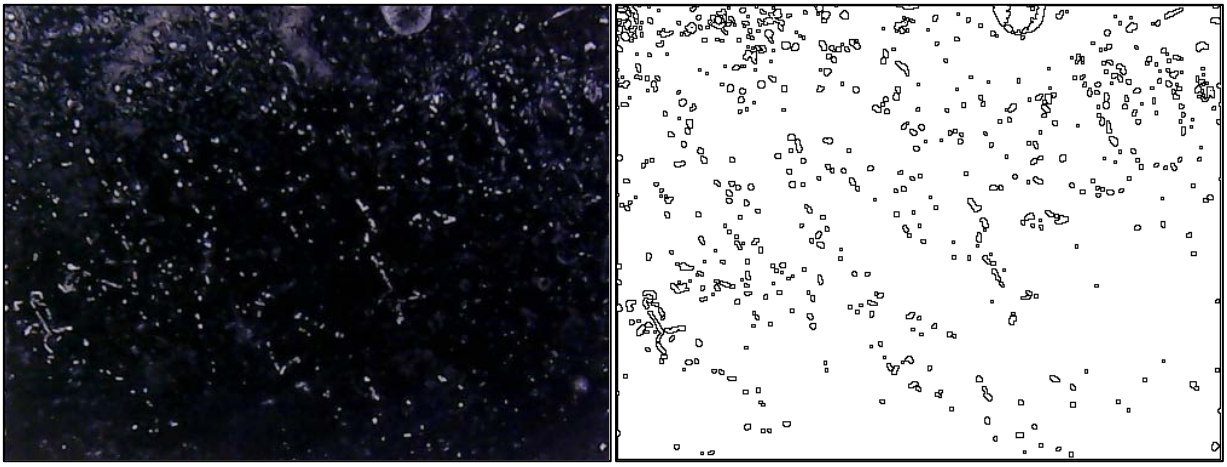

b)

Figure 2. Photographs (left) at 90 minutes of the precipitation of a) NaCl and b) $CaCO_3$, and their corresponding binary images (right)

3.1. Statistical Adjustment of the Observed Results to the Proposed Models

The observed fractal dimension experimental data concerning the area fraction were adjusted by simple regression through equation (25). In contrast, the experimental data related to the evolution of the fractal dimension concerning time were adapted to the model given by equation (26) using Marquardt's nonlinear regression method. For both settings, the STATGRAPHICS software was used.

4. Results and Discussion

In the previous section, the obtaining of a model to describe the morphogenesis of the patterns formed by the evaporative precipitation of salts on a surface is presented.

It is important to point out that the model obtained has limitations (implicit due to the applied formalism):

a) In the first place, the mesoscopic formalism is based on assuming the processes that occur at the microscopic level and their transition probabilities per unit of time, where this assumption is made a priori and not based on the fundamental laws of conservation, where the success in the assumptions depends on the level of knowledge about the process and the experience of the researcher. In this sense, the formalism establishes that the results obtained must be compared with those observed, for which statistical techniques are applied. If there are differences between these, it means that these assumptions are incorrect, and therefore it is necessary to obtain a new model.

b) On the other hand, if a correspondence between these results is obtained, it is necessary to consider that the model parameters are related to the physical and chemical properties of the considered substances, which requires an additional qualitative and logical comparison between the parameters and these properties.

Two parameters are involved in the model presented:

1. The rate constant associated with precipitation k and the rate constant associated with dissolution g, where k may be considered as the intermolecular forces of electrostatic attraction between the ions parameter, while g is related to with the van der Waals forces that exist between the ions and the solvent molecules.
2. Therefore, the k/g ratio expresses the interrelation between these two molecular interaction forces, and it should be expected that an increase in this ratio is related to a lower solubility.

For the model developed in this paper, the results of the adjustments made are shown in Tables 2 and 3. Figure 3 presents the corresponding adjusted models for each experiment. Figure 4 shows the observed temporal behavior of the specific surface area estimated for each experiment and the related trend line in each case.

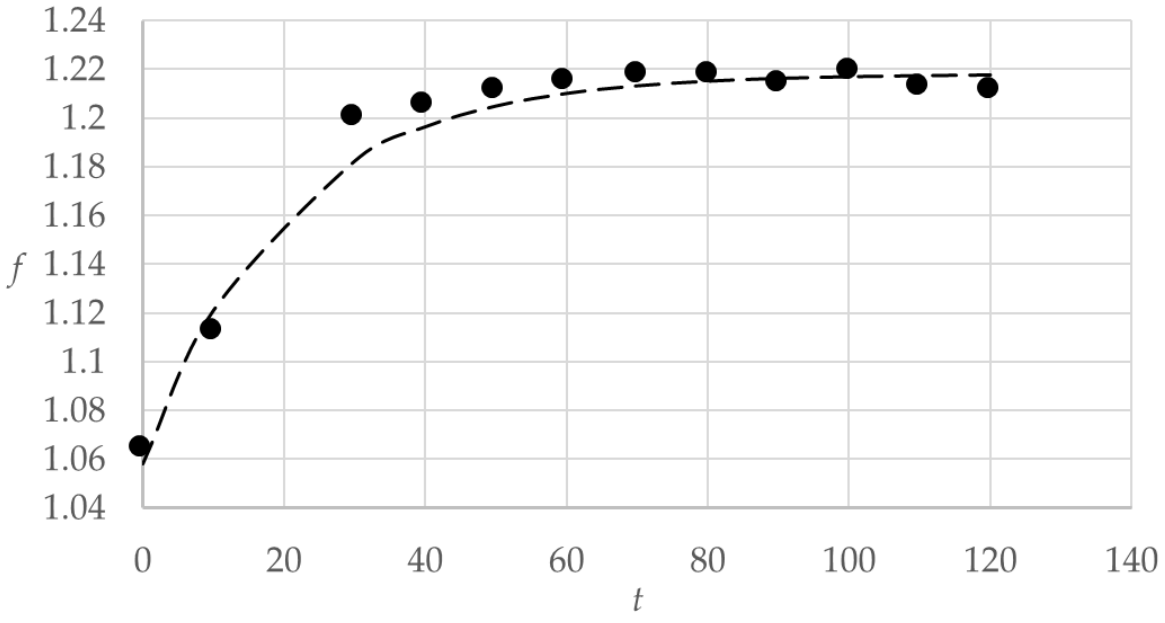

a)

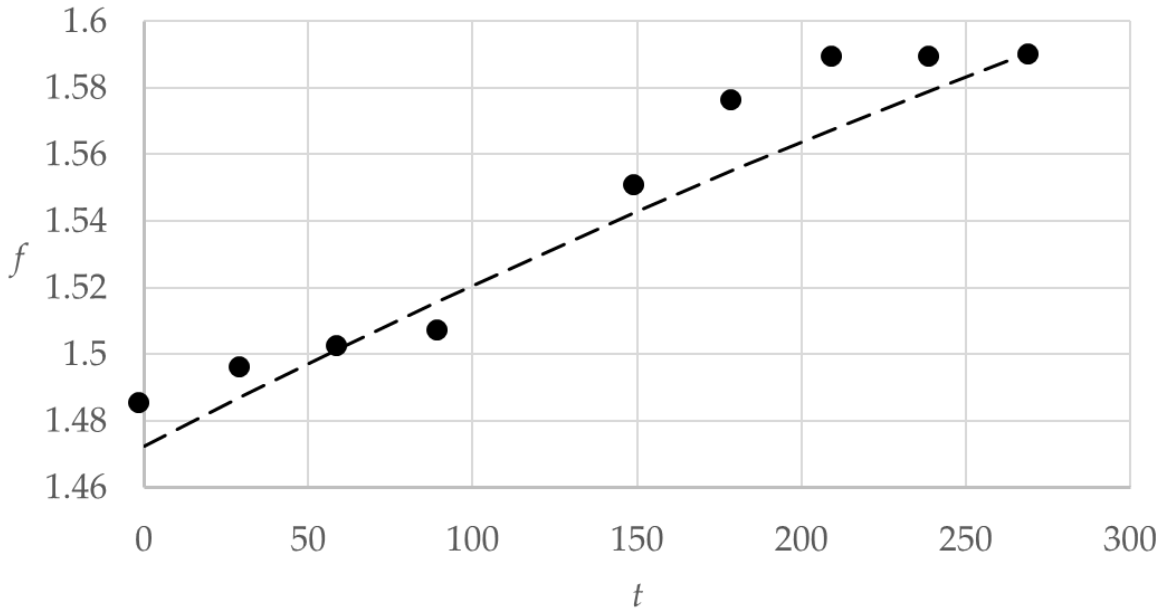

b)

Figure 3. Adjusted model (- - -) and experimental data (●) for a) NaCl and b) $CaCO_3$ precipitates

Table 2. Results of model tuning to experimental data $f = \beta_0 + \beta_1 \Phi$

Parameter	Experiment	Estimation	Error	T	P	
β_0	1 (NaCl)	0.9320	0.0149	62.2108	0.0000	
	2 ($CaCO_3$)	1.2328	0.0131	93.8469	0.0000	
β_1	1 (NaCl)	8.1592	0.463265	17.6125	0.0000	
	2 ($CaCO_3$)	2.5714	0.1076	23.8829	0.0000	
Statistical results		**SS**	**DF**	**SA**	**F**	**P**
Model	1 (NaCl)	0.0263	1	0.0263	310.2000	0.0000
	2 ($CaCO_3$)	0.0142	1	0.0142	570.3900	0.0000
Waste	1 (NaCl)	0.0008	10	0.0000		
	2 ($CaCO_3$)	0.0001	7	0.0000		
Analytical model		**R^2 %**	**R^2 (DF) %**	**SE**	**MAE**	**CC**
Adjustment results	1 (NaCl)	96.8769	96.5646%	0.0092	0.0067	0.9842
	2 ($CaCO_3$)	98.7877	98.6145%	0.0050	0.0035	0.9939
Adjusted model	1 (NaCl)	$f = 0.93 + 8.1592\Phi$				
	2 ($CaCO_3$)	$f = 1.2328 + 2.5718\Phi$				

Nomenclature: **SS:** sum of squares; **DF:** degrees of freedom; **SA:** square average; **F:** mean summary; **CC:** correlation coefficient; **SE:** standard error; **MAE:** Mean Absolute Error

Table 3. Results of model tuning to experimental data $f = \varphi_0 + \varphi_1 \exp(-gt)$

Parameter	Experiment	Estimation	Error	Lowest value	Highest value
φ_0	1 (NaCl)	1.2181	0.0031	1.2109	1.2253
	2 ($CaCO_3$)	1.9055	0.7579	0.0508	3.7602
φ_1	1 (NaCl)	-0.160027	0.00751257	-0.177022	-0.1430
	2 ($CaCO_3$)	-0.4282	0.7523	-2.2692	-1.4126
g	1 (NaCl)	0.0569	0.0069	0.0410	0.0727
	2 ($CaCO_3$)	0.0012	0.0026	0.0051	0.0076
Statistical results		**SS**	**DF**	**SA**	
Model	1 (NaCl)	17.0694	3	5.6898	
	2 ($CaCO_3$)	21.4217	3	7.14056	
Waste	1 (NaCl)	0.0005	9	0.0000	
	2 ($CaCO_3$)	0.0007	6	0.0001	
Analytical model		**R^2 %**	**R^2 (DF) %**	**SE**	**MAE**
Adjustment results	1 (NaCl)	98.0973	97.6745	0.0075	0.0051
	2 ($CaCO_3$)	95.0713	93.4283	0.0115	0.0076
Adjusted model	1 (NaCl)	$f = 1.2181 - 0.1600\, exp(-0.0569t)$			
	2 ($CaCO_3$)	$f = 1.9005 - 0.4282\, exp(-0.0012t)$			

Nomenclature: **SS**: sum of squares; **DF**: degrees of freedom; **SA**: square average; **CC**: correlation coefficient; **SE**: standard error; **MAE**: Mean Absolute Error

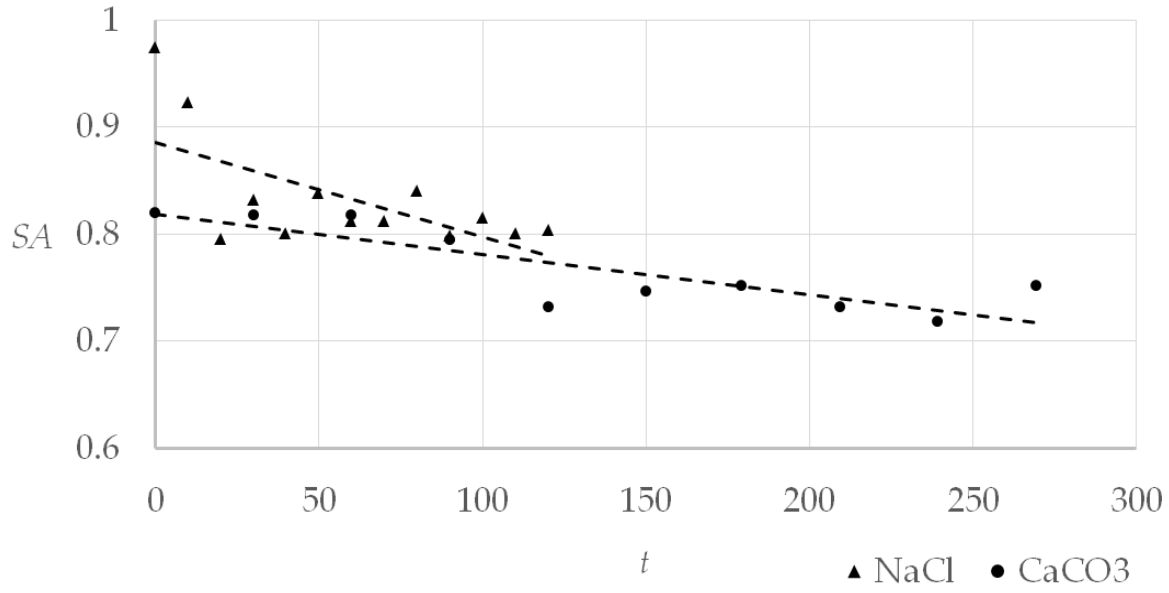

Figure 4. Temporal behavior of the specific surface area (SA) estimated in 2D for each experiment and the corresponding linear trend (- - -)

The results are valid from the statistical point of view, obtaining R^2 values between 95% and 98%, which is acceptable considering the characteristics of these models. The differences observed between the experimental and theoretical results are attributed to three fundamental causes: i) the limitations of the theoretical model established by the initial consideration: the assumption that particles have a constant and the probabilities of transition per unit of time associated with the processes at the microscopic scale; ii) typical errors of the experimental

techniques related to the presence of undetected impurities, fluctuations in environmental conditions and resolution of the photographs of the patterns formed and iii) errors associated with the treatment of the images obtained.

Once obtained and validated from the statistical point of view, the models proceeded to estimate the values of the precipitation rate and dilution constants of the salts. From equations (27) and (28), considering that M_0 is proportional to the initial salt concentration, it is calculated that the maximum fraction of the surface covered by the precipitate is obtained when practically all the solvent has evaporated. Table 4 presents the estimated values of the precipitation and dissolution rate constants calculated using equations (27) and (28) and the maximum observed value of covered area when time tends to infinity.

Table 4. Precipitation and dissolution rate constants estimated from the model and solubility of each salt

Salt	Φ_0	M_0	k	g	k/g	Solubility g/l
NaCl	0.0549	0.0354	0.0566	0.0569	0.9951	350
$CaCO_3$	0.0931	0.1356	0.0022	0.0012	1.9147	0.013

The solubility of salt in water is defined as the amount of salt that can be dissolved so that while the solubility is higher, a higher concentration of salt is necessary for precipitation to take place. In other words, for the same solvent, it is easier for the precipitation of compounds that have a lower solubility to occur in it. In this sense, this property depends on the nature of the salt and the molecular interactions that are established between the solute and the solvent. From the results in Table 4, it can be suggested that calcium carbonate salt precipitates more easily than sodium chloride salt since its solubility is significantly lower. This result is observed experimentally, where the maximum fraction of the covered surface was found for experiment 2, even though the concentration used was lower than the saturation of this compound and lower than that corresponding to experiment 1, where a saturated solution was prepared.

On the other hand, the dynamics associated with the precipitation process is influenced by different factors related to the ion transport processes, the precipitation and dissolution of the precipitated particles, the size of the particles, and the initial concentration of the salt. According to equation (26), the time required for the system to achieve the steady-state is proportional to the inverse of the dissolution rate. As this velocity increases, the system will reach this state faster. Dissolution is a phenomenon that takes place on the particle's surface, in such a way that the velocity increases as the specific surface area of the particle increases. This is manifested in the fact that the dissolution rate constant of an individual particle is proportional to its specific surface area, so the size of the particles and how it evolves influences the dissolution rate constant g of the system. According to Figure 4, the specific surface area of the NaCl particles is greater than that corresponding to the $CaCO_3$ particles, so in the first case, it is expected that the dissolution rate g will be greater, as predicted by using the adjustment of the proposed model for the estimation of this parameter (Table 4). Note further that for both experiments, the specific surface area of an individual particle decreases over time, indicating that the average size increases and is expected in crystallization and precipitation.

Although the dynamics of the pattern formation process is influenced by the average particle size and dissolution rate, the steady-state that is reached, which depends on the principles of thermodynamics and statistical thermodynamics, will depend on both: the solubility of the salts and the k/g ratio between the crystallization and dissolution rate constants in the state close to thermodynamic equilibrium. In this case, it is reasonable to expect that an increase in the k/g ratio will lead to a decrease in the solubility of the system. This is reflected in Table 4, where, in the case of calcium carbonate, the solubility is significantly lower than that corresponding to sodium chloride, obtaining that its quotient k/g estimated from the proposed model practically duplicates the sodium chloride k/g.

Other studies can be considered as [20] for the cuboidal regions' places. In this paper a salt deposition is a phenomenon that can lead to problems in the industry, as salts deposited on the surface of pipe and equipment affect the processes of fluid transport and heat transfer. This phenomenon can also cause problems in building structures when the foundations are embedded in substrates that are in contact with groundwater with a high salt content due to the proximity of marine coasts. Studies related to the physiochemistry, and kinetics of these phenomena are useful to quantify the effectiveness of the treatments that are carried out to mitigate their effects, and that can be related to the injection of chemical additives, better treatment of water as a raw material or an improvement in the properties of the surfaces on which a significant deposition of salts can occur. In this sense, the mathematical model and the proposed methodology can contribute to deepening these studies.

5. Conclusions

Considering the microscopic processes in precipitation and re-dissolution of salts occurring with a certain probability, a mesoscopic stochastic model was obtained to describe the behavior of the area fraction covered by salts precipitated by evaporation and the variance associated with internal fluctuations that reflect the influence of microscopic processes on the pattern. Based on this model and considering the principles of fractal geometry, an equation is proposed to describe the temporal behavior of the fractal dimension of the spatial patterns that form precipitated particles. The proposed model was used to study the precipitation of sodium chloride (supersaturated

solution) and calcium carbonate (low solubility). From the adjustment of the proposed models to the observed experimental data, the value of the velocity constants of the precipitation and dissolution processes was estimated. In this case, it was found that the dissolution rate is higher in the case of sodium chloride, which has greater solubility, and particles with a specific surface area greater than carbonate salts were formed. On the other hand, the ratio between the precipitation rate constant and the dissolution rate constant is higher as the solubility of the salt decreases (in this case it is almost double for sodium carbonate, which has a significantly lower solubility compared to sodium chloride). This result is expected and reasonable if solubility measures a solute's ability to dissolve in each solvent.

Acknowledgments

EJSD and RRGV thank PRODEP for the support for the project to "*Fortalecimiento de cuerpos académicos* 2021" (FADU-UAT). JFPS appreciates the support of the CONACYT Project Number 321258. Equipment used in this research was obtained due CONACYT Project 316443 and 54-UATINVES21.

Funding

PRODEP 2021 and CONACYT 315372.

Conflicts of Interest

The authors declare no conflict of interest.

REFERENCES

[1] Lee, C., Naing, N.C. P., Herrera, D., Aguirre, G., Rodriguez, B., & Ashcroft, J. Light up My Life: An Active Learning Lab to Elucidate Conductive Properties of Electrolytes. *Journal Of Laboratory Chemical Education*, 2019. *7*(1), 1-7.

[2] Zavitsas, A. A. Properties of aqueous solutions. A treatise against osmotic and activity coefficients. *Journal of Molecular Liquids*, 2022, *348*, 118410.

[3] Gongadze, E., Mesarec, L., Kralj-Iglic, V., & Iglic, A. The asymmetric finite size of ions and orientational ordering of water in electric double layer theory within lattice model. *Mini-reviews in medicinal chemistry*, 2018, *18*(18), 1559-1566.https://doi.org/10.2174/1389557518666180626111927

[4] Cohen, P. (editor), The ASME Handbook on Water Technology for Thermal Power Systems, The American Society of Mechanical Engineers, 1989.

[5] Luo, T., Abdu, S., & Wessling, M. Selectivity of ion exchange membranes: A review. *Journal of membrane science*, 2018, *555*, 429-454. https://doi.org/10.1016/j.memsci.2018.03.051

[6] Bánhegyi, D. F., & Pálovics, E. The Stoichiometry, structure and possible formation of crystalline diastereomeric salts. *Symmetry*, 2021, *13*(4), 667.

[7] Gupta, S. K., & Mao, Y. Recent developments on molten salt synthesis of inorganic nanomaterials: A review. *The Journal of Physical Chemistry C*, 2021, *125*(12), 6508-6533. https://doi.org/10.1021/acs.jpcc.0c10981

[8] Nakamuro, T., Sakakibara, M., Nada, H., Harano, K., & Nakamura, E. Capturing the moment of emergence of crystal nucleus from disorder. *Journal of the American Chemical Society*, 2021, *143*(4), 1763-1767.

[9] Alipour, A., Abedi, M., & Habibi, M. Controlling salt crystallization in evaporating thin films of colloidal liquids. *Colloids and Surfaces A: Physicochemical and Engineering Aspects*, 2022, *636*, 128094.

[10] Cui, K., Zhao, X., Hu, M., Yang, C., & Xie, G. Effect of Salt Content on the Evaporation and Cracking of Soil from Heritage Structures. *Advances in Materials Science and Engineering*, 2021, *2021*.

[11] Li, D., Yang, B., Yang, C., Zhang, Z., & Hu, M. Effects of salt content on desiccation cracks in the clay. *Environmental Earth Sciences*, 2021, *80*(19), 1-13. https://doi.org/10.1007/s12665-021-09987-8

[12] Ting, M. Z. Y., Wong, K. S., Rahman, M. E., & Meheron, S. J. Deterioration of marine concrete exposed to wetting-drying action. *Journal of Cleaner Production*, 2021, *278*, 123383. https://doi.org/10.1016/j.jclepro.2020.123383

[13] Luo, Y., Zhou, P., Ni, P., Peng, X., & Ye, J. Degradation of rammed earth under soluble salts attack and drying-wetting cycles: The case of Fujian Tulou, China. *Applied Clay Science*, 2021, *212*, 106202.

[14] Ftameh Khaled, Pah Chin Hee, "On Three-Dimensional Mixing Geometric Quadratic Stochastic Operators," Mathematics and Statistics, Vol. 9, No. 2, pp. 151-158, 2021. DOI: 10.13189/ms.2021.090209.

[15] Hellander, S., Hellander, A., & Petzold, L. Reaction-diffusion master equation in the microscopic limit. *Physical Review E*, 2012, *85*(4), 042901.

[16] Zhou, Y., & Zuo, W. Density function and stationary distribution of a stochastic SIR model with distributed delay. *Applied Mathematics Letters*, 2022, 107931. https://doi.org/10.1016/j.aml.2022.107931

[17] Van Kampen, N. G. (1992). *Stochastic processes in physics and chemistry* (Vol. 1). Elsevier. ISBN 0-444-89349-0

[18] Suarez-Dominguez, E. J., Xu, B., Perez-Sanchez, J. F., Palacio-Perez, A., & Izquierdo-Kulich, E. (2018). Stochastic modeling of asphaltenes deposition and prediction of its influence on friction pressure drop. *Petroleum Science and Technology*, *36*(21), 1812-1819. https://doi.org/10.1080/10916466.2018.1514406

[19] Mandelbrot, B. B. (1986). Self-affine fractal sets, I: the basic fractal dimensions. In *Fractals in physics* (pp. 3-15). Elsevier.

[20] Brenda Mbouamba Yankam, Abimibola Victoria Oladugba, "Prediction Variance Capabilities of Third-Order Response Surface Designs for Cuboidal Regions," Mathematics and Statistics, Vol. 9, No. 5, pp. 760-772, 2021. DOI: 10.13189/ms.2021.090516.